

Review

Mapping Palaeohydrography in Deserts: Contribution from Space-Borne Imaging Radar

Philippe Paillou

Laboratoire d'Astrophysique de Bordeaux, Université de Bordeaux, UMR 5804-CNRS, 33600 Pessac, France; philippe.paillou@u-bordeaux.fr

Academic Editor: Frédéric Frappart

Received: 20 January 2017; Accepted: 5 March 2017; Published: 8 March 2017

Abstract: Space-borne Synthetic Aperture Radar (SAR) has the capability to image subsurface features down to several meters in arid regions. A first demonstration of this capability was performed in the Egyptian desert during the early eighties, thanks to the first Shuttle Imaging Radar mission. Global coverage provided by recent SARs, such as the Japanese ALOS/PALSAR sensor, allowed the mapping of vast ancient hydrographic systems in Northern Africa. We present a summary of palaeohydrography results obtained using PALSAR data over large deserts such as the Sahara and the Gobi. An ancient river system was discovered in eastern Lybia, connecting in the past the Kufrah oasis to the Mediterranean Sea, and the terminal part of the Tamanrasset river was mapped in western Mauritania, ending with a large submarine canyon. In southern Mongolia, PALSAR images combined with topography analysis allowed the mapping of the ancient Ulaan Nuur lake. We finally show the potentials of future low frequency SAR sensors by comparing L-band (1.25 GHz) and P-band (435 MHz) airborne SAR acquisitions over a desert site in southern Tunisia.

Keywords: SAR; radar; deserts; palaeohydrography; Sahara; Gobi

1. Introduction

Space-borne Synthetic Aperture Radar (SAR) allows the mapping of continental surfaces at centimetre-scale wavelengths. It is an active remote sensing technique, producing high resolution images sensitive to surface topography and roughness, and to soil water content [1]. In very dry soils, SAR is able to probe the subsurface down to several meters: it was shown that L-band (1.25 GHz) radar is able to penetrate meters of low electrical loss material such as sand [2,3]. Thanks to the first Shuttle Imaging Radar SIR-A mission, McCauley et al. [4] demonstrated radar subsurface imaging capabilities for a site located in the Selima Sand Sheet, in southern Egypt. Radar images revealed buried and previously unknown palaeodrainage channels (see Figure 1), which afterwards were confirmed by field studies [5,6]. Later in 1995, SIR-C radar was used to map the subsurface basement structures that control the Nile's course in northeastern Sudan [7]. More recent studies have shown that combining Shuttle Radar Topography Mission (SRTM) data [8] with SAR images better reveals subsurface features that still present a topographic signature. New palaeodrainage flow directions have thus been mapped in eastern Sahara [9], allowing better definition of drainage lines leading to oases and valleys, as well as a better mapping of the past aquifers [10,11].

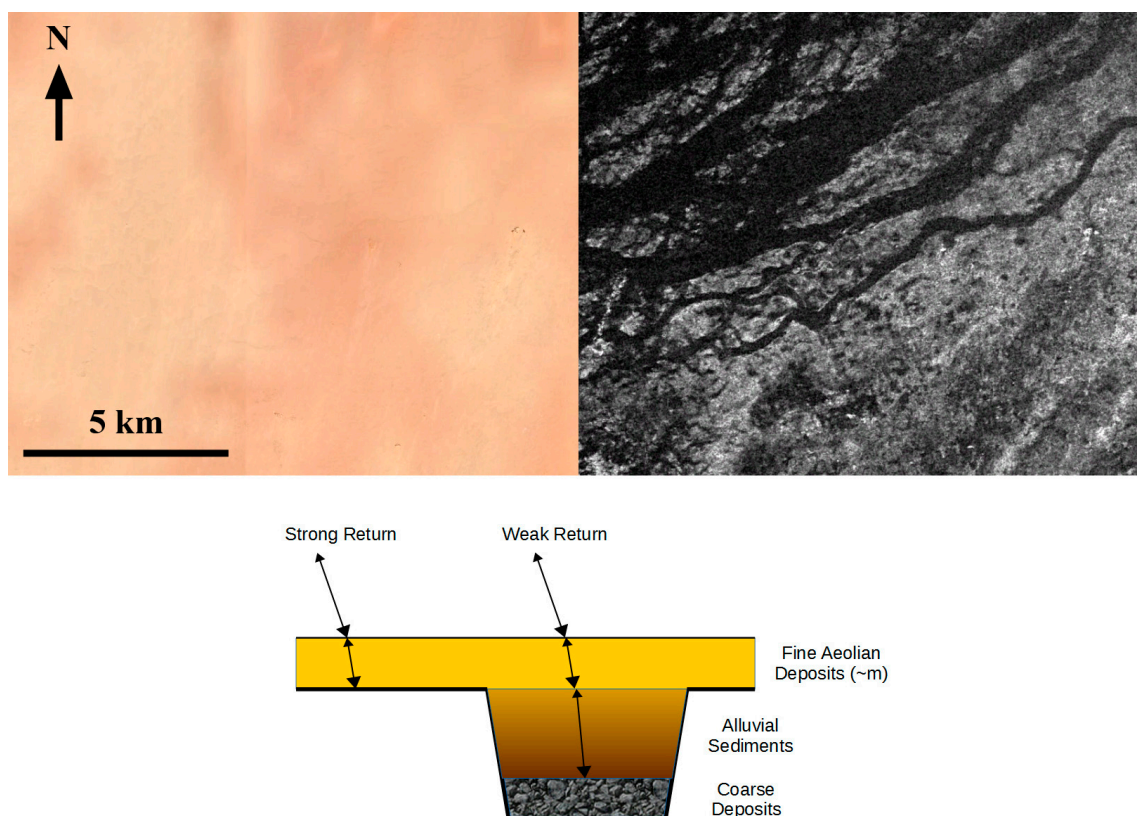


Figure 1. (Top left) SPOT (Satellite Pour l’Observation de la Terre) image of part of the Selima Sand Sheet located in southern Egypt (22.55° N–29.28° E). (Top right) Radar image from Japanese polarimetric L-band synthetic aperture radar (PALSAR) of the same area, revealing numerous palaeochannels hidden by a meter-thick layer of aeolian sand. (Bottom) Sketch of radar wave interaction with surface sand, subsurface bedrock and palaeochannel. The radar wave is absorbed by the alluvial sediments, leading to a weak return, while it is backscattered by the rough bedrock under the thin sand cover, leading to a stronger return.

While the geographical coverage of the Shuttle Imaging Radar missions was limited, a more complete L-band radar coverage of the eastern Sahara was acquired by the JERS-1 satellite of the Japanese space agency (JAXA). It was used to produce the first regional-scale radar mosaic covering Egypt, northern Sudan, eastern Libya, and northern Chad. This data set helped discover numerous unknown crater structures in eastern Sahara [12]. Later in 2006, JAXA successfully launched the Advanced Land Observing Satellite (ALOS), carrying a full polarimetric L-band SAR, named PALSAR, which offered higher resolution imagery and a much improved signal to noise ratio as compared to JERS-1 [13]. Full coverage of the Sahara and Arabia was acquired during June and July 2007, delivering more than 400 PALSAR strips at a resolution of 50 m (see Figure 2). A fully automated data processing chain allowed to produce geocoded $1^\circ \times 1^\circ$ SAR scenes that can be superposed to the corresponding $1^\circ \times 1^\circ$ SRTM squares, covering latitudes between 17° N and 37° N and longitudes between 17° W and 60° E. The whole dataset is managed with the help of a web map server, allowing the import and display of PALSAR data using Google Earth. It is freely accessible through a dedicated web site [14]. This PALSAR dataset constitutes a unique tool for the scientific community to study the palaeo-environment and palaeoclimate of North Africa and Arabia. It also helps in the building of more complete geological maps and in support of future water prospecting in arid and semi-arid regions [15]. Recently, the PALSAR dataset was extended to the Gobi Desert in Central Asia, covering latitudes between 34° N and 52° N and longitudes between 73° E and 120° E.

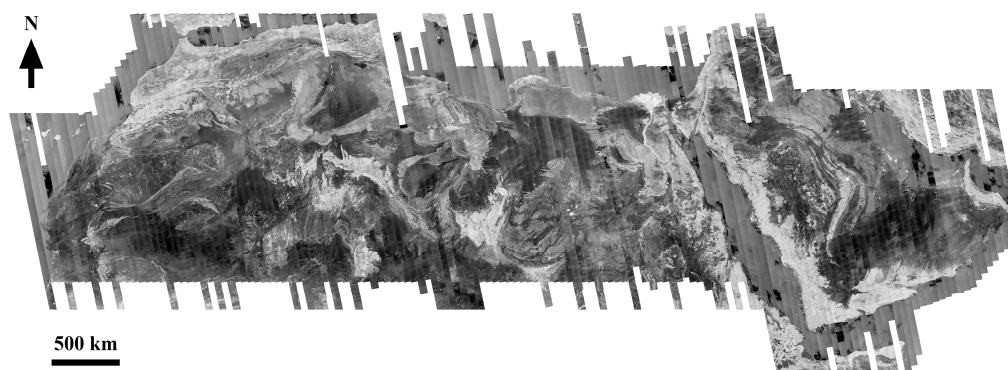


Figure 2. PALSAR strips acquired by the Japanese space agency (JAXA) over the Sahara and Arabia during the summer of 2017.

2. Case Studies Using PALSAR L-Band Sensor

2.1. The Kufrah Palaeoriver in Eastern Sahara

Many of the major drainage basins in North Africa were influenced by the Messinian salinity crisis in the late Miocene, when desiccation of the Mediterranean Sea promoted deep landscape incision. In central Sahara, extensive drainage systems originating in the Tibesti mountains were flowing northward to the Mediterranean Sea and southward to the Chad Basin. While this region is now hyperarid, remains of past river systems have been detected using remote sensing imagery, leading some authors to propose palaeodrainage pathways between south Libya and the Mediterranean Sea [9,16].

For the first time, PALSAR L-band images allowed an accurate mapping of a continuous 900 km-long palaeodrainage system, named the Kufrah River (see Figure 3). Its headwaters are mainly in southern Libya with observed tributaries arising in three main areas: El Fayoud and El Akdamin hamadas in northeastern Tibesti (Wadi Al Kufrah), northern Uweinat close to the Sudanese border (Uweinat tributary), and the western Gilf Kebir and Abu Ras plateaux on the Egyptian border [17]. The end of the Kufrah River disperses as a network of small shallow channels across the surface of the broad Sarir Dalmah alluvial fan, that covers more than 15,000 km², possibly constituting an inland delta. It is not possible to follow the river course to the north because the large and thick sand dunes of the Calanscio Sand Sea preclude radar mapping of the subsurface. However, about 300 km away to the northwest and emerging from beneath the Calanscio Sand Sea, lies the major, 2 to 4 km-wide, alluvium-filled Wadi Sahabi palaeochannel that incised more than 300 m into bedrock. Analysis of SRTM topography combined with PALSAR scenes allowed the mapping of several additional palaeochannels located west of the Kufrah River, each of which is likely to have formed a tributary that supplied water and sediment to the main palaeodrainage system. SRTM topography also revealed local depressions which allow to connect the western palaeochannels and the terminal alluvial fan of the Kufrah River to the Wadi Sahabi palaeochannel, through a 400 km-long palaeocorridor [18].

The Kufrah River is then a major palaeodrainage system in eastern Sahara, which at its maximum extent would have drained an area of more than 400,000 km² between the Tibesti, Al Haruj, and Gilf Kebir massifs and connected to the Mediterranean Sea in the Sirt Basin through the Wadi Sahabi palaeochannel, possibly discharging a comparable amount of water as does the present-day Nile. Despite the fact we have no direct indication about the age of initiation and history of the Kufrah River, it is very likely to have been active during recent (Holocene) times as proposed by Pachur and Altmann [19]: even though L-band radar does not allow to see deeper than a couple of meters, the palaeochannels are clearly visible in PALSAR images, suggesting that they are only at shallow depths. Earlier (Pleistocene) phases of activity are also likely: Osborne et al. [20] proposes a “humid corridor” that was connecting the Kufrah Basin to the Mediterranean coast 120,000 years ago. The Kufrah River system is then clearly a major palaeohydrological feature to take into account when studying the

past environments and climates of northern Africa, from the middle Miocene to the Holocene. It also represents a likely corridor for fauna and human dispersal in the eastern Sahara, and thus indicates locations where further palae-ontological, palae-anthropological, and archaeological field exploration should be conducted.

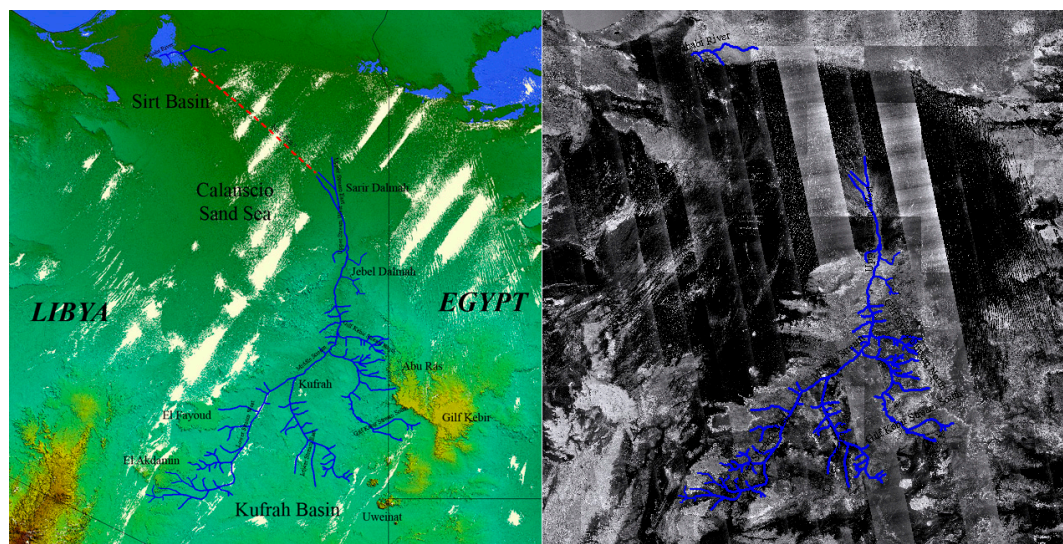


Figure 3. The Kufrah palaeoriver system (in blue) on top of Shuttle Radar Topography Mission (SRTM) topography (**left**) and on top of the PALSAR mosaic (**right**). The red dash line indicates a possible corridor connecting the terminal fan of the Kufrah River to the Mediterranean coast, through the Wadi Sahabi palaeochannel.

2.2. The Tamanrasset Palaeoriver in Western Sahara

The Green Sahara Periods (GSPs) are due to astronomically related changes and are the consequence of the transformation of the hydrological cycle over North Africa, with the intensification of the African summer monsoon. Changes in the position of this rain belt led to development of important fluvial networks over the Sahara, which resulted in an increase of freshwater delivery to surrounding oceans. Marine sediment records from the Mediterranean and Atlantic margins have provided consistent evidence of monsoon variability in northern Africa since the middle Pleistocene. The most recent GSP, which spans from 12,000 to 5000 years BP, is commonly referred to as the early Holocene African Humid Period (AHP). It is well recorded in marine sedimentary archives from the Gulf of Guinea to the northeastern Tropical Atlantic Ocean, the Mediterranean margin, and eastern Africa.

Off the western African margin, fluvial signals have been identified in deep-sea sediments dated from the early Holocene [21]. Recently, a large 400 km-long submarine channel system, the Cap Timiris Canyon, has been discovered on the western Sahara margin off Mauritania [22]. The Cap Timiris Canyon was very likely connected to a major river system in the past, and potential flow pathways simulated from present-day topography indicates the existence of a large river system in western Sahara, taking its sources in the Hoggar highlands and the southern Atlas Mountains. This so-called Tamanrasset River valley has been described as a possible vast and ancient hydrographic system [23]. Although a possible link between the Tamanrasset River and the Cap Timiris Canyon has already been suggested, no direct evidence of any fluvial activity and of a connection to the canyon has ever been found. PALSAR images of the Mauritanian coast provide geomorphological evidence for the existence of a palaeodrainage system located in the Arguin Bay, between Cap Blanc and Cap Timiris (see Figure 4). This newly identified palaeodrainage system is about 500 km-long and overlaps very well with the coastal section of the course of the Tamanrasset River inferred from topography. The reconstruction of the complete system was not possible using PALSAR images, due to the presence

of thick sand dunes. However, the branch of the palaeodrainage network identified using radar represents a fifth of the total length of the Tamanrasset palaeoriver. The palaeochannels detected in radar images are also perfectly aligned with palaeovalleys identified in the Arguin Basin, as well as with the proximal tributaries of the submarine Cap Timiris Canyon system [24].

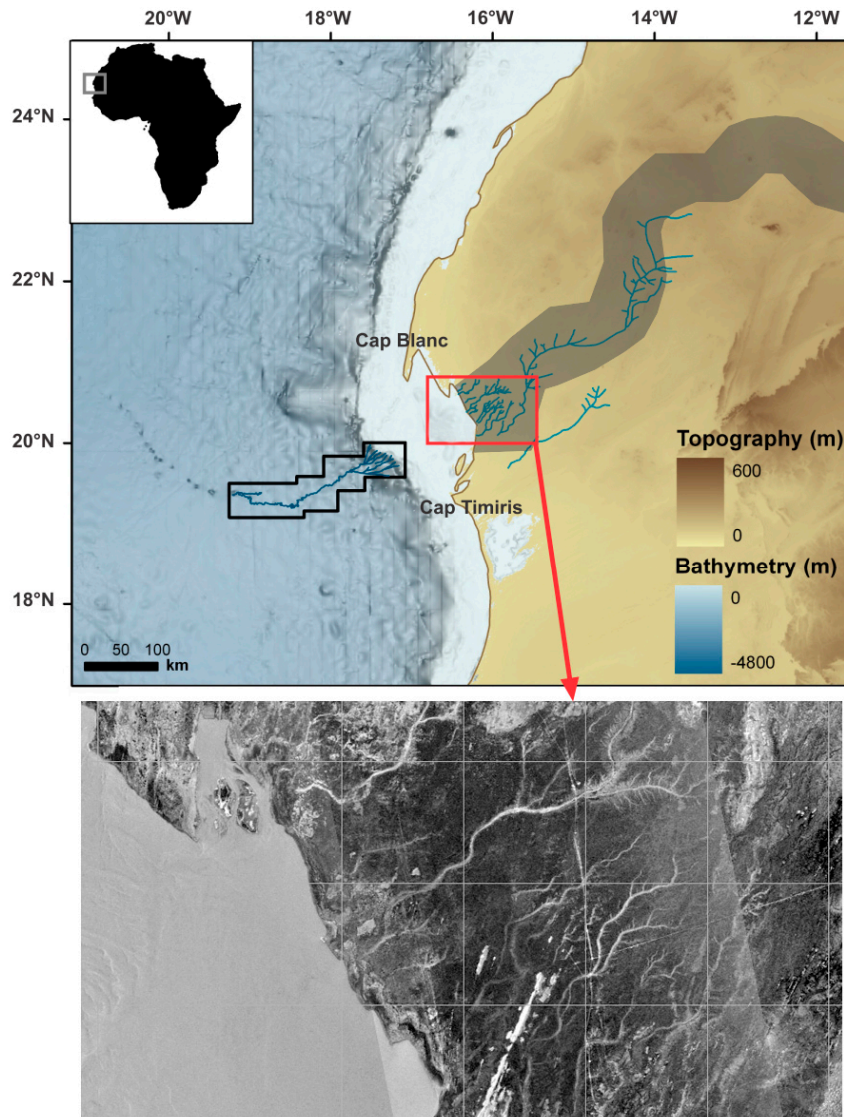


Figure 4. (Top) Topographic map of Mauritanian coast, showing locations of the Timiris Canyon (black square), palaeochannels detected in PALSAR data (blue lines) and Tamanrasset River valley (dark brown area), after [24]. (Bottom) PALSAR mosaic showing the discovered palaeodrainage system. “Radar rivers” appear here as bright features, due to the accumulation of coarse gravels in the terminal part of the channels, producing a higher radar return.

Thanks to orbital space-borne imaging radar, it was possible to establish the continuity of a past giant drainage system in western Africa, from the continent (Tamanrasset River) to the shelf (Arguin basin), and then to the bottom ocean (Cap Timiris Canyon). Overall, the identification of this palaeodrainage system in the Arguin Bay area is very coherent with the hydrological landscape of the western Sahara, especially during the most recent GSPs. The evidence of a fluvial activity on the Mauritanian coast during the recent past provides a missing link between the development of lakes over Algeria and Mauritania and fluvial evidences in Algeria. The presence of a vast fluvial system in the past in the place of present-day major dust sources also provides a new light on the

interplay between aeolian and fluvial supplies in the making of the terrigenous signal off western Africa. This finding also provides valuable constraints for numerical simulations of Saharan climate throughout the late Quaternary.

2.3. The Ulaan Nuur Palaeolake in Central Asia

Arid Inner Asia has experienced dramatic climate fluctuations over the last millennia [25] and remains highly sensitive to ongoing climatic change. As a consequence, lakes in the Gobi Desert underwent major level changes during the Late Quaternary, with high stages being associated with wetter climates. The early Holocene in Mongolia is characterized by increasing temperature and humidity, followed by a humid early-mid Holocene stage, when lakes were at high volume. Enhanced aridity occurred during the mid-Holocene, but the beginning and end of the dry interval differs from location to location. In the late Holocene the humidity increased due to decreased evaporation when temperatures dropped in Mongolia. Due to its location, Mongolia is influenced by both the North Atlantic Oscillation and the East Asian Monsoon, associated with El Niño effect, making the region an important source for establishing Holocene climatic signals [26].

Remains of past wetter climates can be found in today's topography in the form of palaeochannels and palaeoshorelines, in particular in the desert of southern Mongolia [27,28]. We studied the Ulaan Nuur depression (44.53° N–103.73° E), located in a large and flat expanse in the Omnogov province, which was in the recent past the southern terminus for the Ongi River. We conducted the analysis of present-day topography provided by SRTM data, coupled with PALSAR imaging. PALSAR allowed the mapping of palaeochannels and palaeofans of ancient rivers feeding the Ulaan Nuur depression, while SRTM topography was used to simulate various palaeolake levels and map the location of possible palaeoshorelines [29]. We actually identified ten potential palaeochannels, strongly indicative of watercourses feeding Ulaan Nuur in the past. Two main streams are represented by the Ongi River (Figure 5A) and a southeastern channel (Figure 5C) that correspond to strong incision in the bedrock. They appear as bright linear structures in PALSAR images, because coarse alluvial gravel filling the channel bed increase the surface roughness and volume scattering effects, leading to a strong radar return. Secondary tributaries also appear to have fed the Ulaan Nuur depression from the northwest, but with a somewhat less important water flow, creating numerous alluvial fans (Figure 5B). Palaeoshoreline morphologies can be clearly observed in present day topography: the Ulaan Nuur depression is bordered by wave-cut terraces in the north (Figure 5D) and in the south (Figure 5E,F).

The observed terraces actually form sequences that can be accounted for by varying lake levels. Figure 5 shows three main lake levels that we reconstructed by artificially flooding the present-day topography, choosing water levels in order to match the observed palaeoshorelines and channel fans. The bigger outer lake covers an area of 19,500 km² and is limited in the south by a sharp west-east trending palaeoshoreline. It also corresponds in the north to the limit where the Ongi River flows out of higher relief, and shows a bed transition from narrow to wide, indicating that the flow competence has declined markedly downstream. A medium-size lake, corresponding to a surface of about 6900 km², can then be defined and limited by northwestern and southeastern alluvial fans and shorter palaeoshorelines. The intermediate-size lake is likely to have been fed by low competence flows from the northwest and from the southeast, which left numerous, and wide alluvial fan remnants. It is coherent with a decrease in water level, since the Ongi River also becomes less competent between the large and medium lake limits, as shown by a wider and shallower bed morphology. Finally, a small-size lake, probably the most recent one, occupied an area close to 1700 km² and was limited in the north by a plateau and by being the termination of all mapped palaeochannels, including the present day Ongi River. This is likely to have been the final stage of the Ulaan Nuur, by the end of the progressive drying Holocene phase, before the present-day dry and desiccated depression.

Considering the surface area covered by the bigger extent of Ulaan Nuur lake, and taking the present day topography as lake floor, we estimated that an amount of more than 3000 km³ of fresh water was present in the past, filling the Ulaan Nuur depression. Considering the Holocene

palaeoclimatology of southern Mongolia, this lake is likely to have last several thousands of years, leading to significant amount of water infiltrating in the shallow subsurface. This suggests that shallow water resources may be located at multiple sites in the Ulaan Nuur depression: this is a suitable resource for small-scale community, accessible using inexpensive shallow drilling techniques.

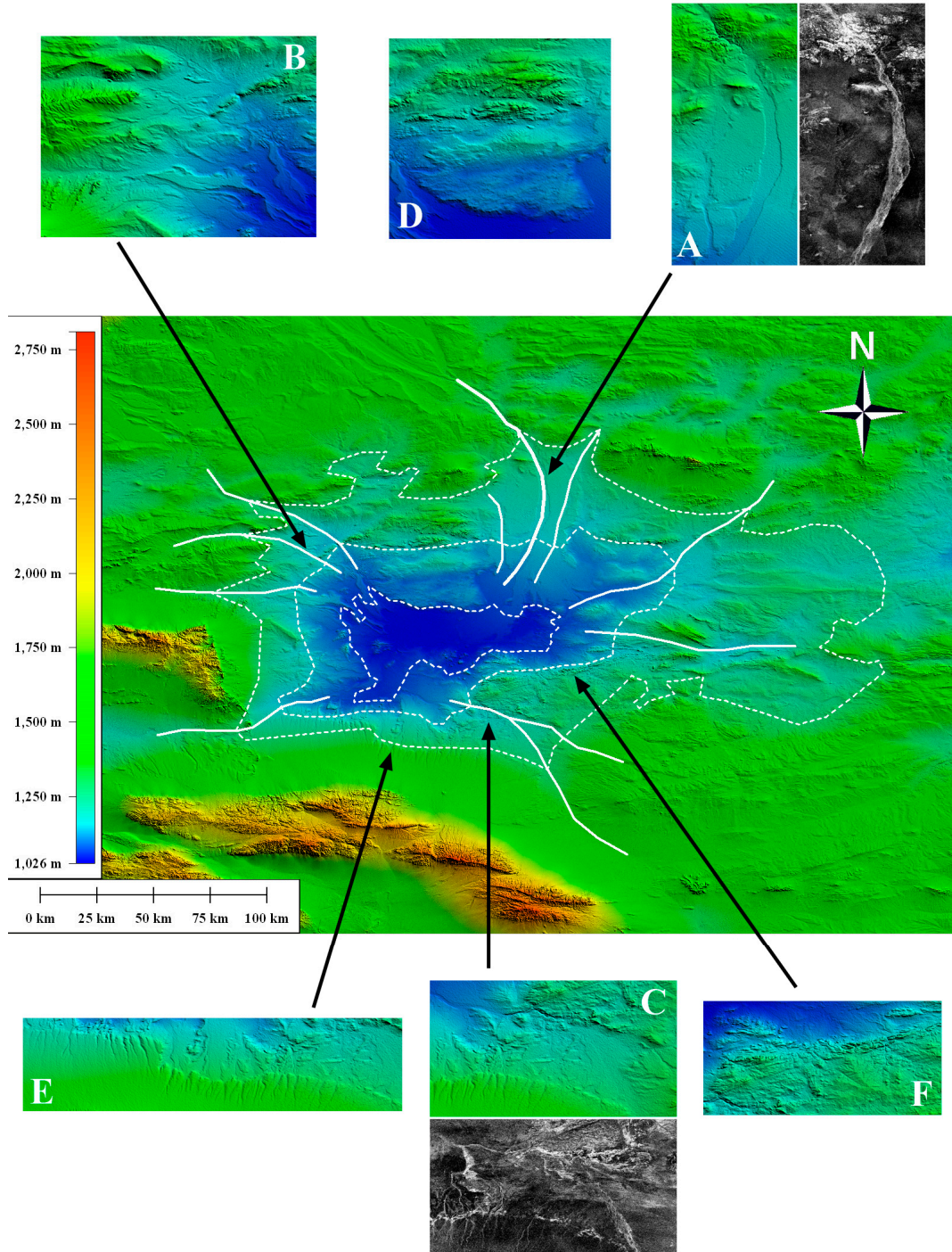


Figure 5. Ulaan Nuur depression on top of SRTM topography, showing the three past lake levels (dotted white lines) and the ten palaeochannels (solid white lines). Ulaan Nuur’s main streams are the Ongi River (A) and a southeastern channel (C). Terminal fans of secondary tributaries (B) and palaeoshoreline morphologies (D–F) remain visible in the present day topography.

3. The Future of Space-Borne Imaging Radar: Low Frequency Sensors

Previous cases have shown the benefit of using L-band space-borne imaging radar for mapping the shallow subsurface in arid environments: even a shallow investigation depth of a couple of meters is enough to obtain significant and new information about palaeohydrography. An easy way to probe the subsurface deeper is to go for longer radar wavelengths: while a L-band (1.25 GHz) radar can penetrate 1–2 m of dry sand, a P-band system (435 MHz) should be able to probe the subsurface down to more than 5 m [30]. In June 2010, we conducted an airborne P-band SAR campaign over a desert site in southern Tunisia, using the SETHI system developed by ONERA [31]. This is the first time a low frequency P-band radar was flown over the Sahara. We acquired several radar scenes over the Ksar Ghilane oasis (32.98° N–9.63° E), an arid area at the limit between past alluvial plains and present day sand dunes. Figure 6 shows the comparison between a L-band radar scene acquired by the ALOS-2 Japanese sensor and a P-band radar scene acquired by the SETHI system: P-band radar better reveals the subsurface features under the superficial sand layer because of its higher penetration depth. A lower frequency radar is also less sensitive to the covering sand surface, leading to a lower contribution of the superficial layer. Using a two-layers scattering model for the surface and subsurface geometry shown in Figure 1, we could reproduce both the L- and P-band measured scattering levels, which are actually comparable. At L-band, the subsurface layer produces a backscattering component about 30 times lower than the one produced by the surface layer, while at P-band, the subsurface layer contribution is about thirty times higher than the surface layer component. The lower surface scattering term at P-band, due to a smoother surface roughness at a longer wavelength, is balanced by a higher subsurface scattering term, due to a higher penetration depth. As a final result, the total scattering level at P-band is comparable to the one at L-band, as observed by ALOS-2 and SETHI sensors, but the P-band return is dominated by the subsurface layer [32].

This indicates that a space-borne P-band SAR should be able to very efficiently map subsurface geological and hydrological features in arid areas. In 2021, the European Space Agency will launch its seventh Earth Explorer mission, named BIOMASS [33]. It is being designed to provide, for the first time from space, P-band SAR measurements to determine the amount of biomass and carbon stored in forests by combining a low radar frequency, polarimetric, interferometric, and tomographic techniques. It will also, as a secondary objective, map the subsurface geology in large desert regions such as the Sahara, Central Asia, and Australia. The BIOMASS mission will then offer a unique opportunity to reveal the hidden and still unknown past history of deserts.

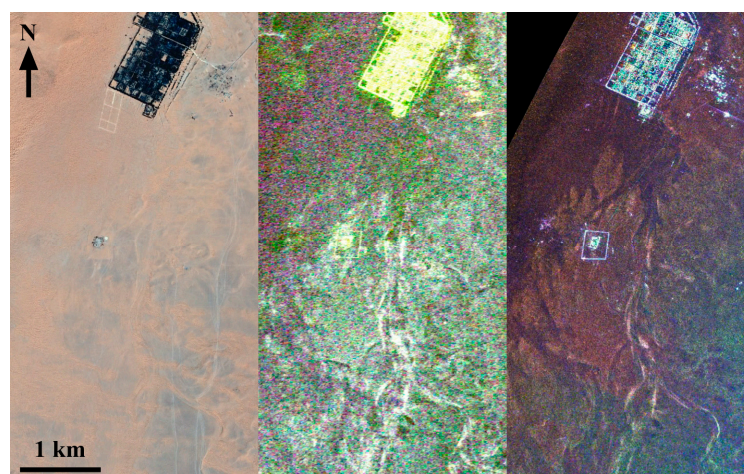


Figure 6. (Left) SPOT image of the Ksar Ghilane oasis region in southern Tunisia, palaeochannels are hidden by aeolian sand deposits. (Middle) ALOS-2 L-band radar image, showing some subsurface features still blurred by the radar return of the superficial sand layer. (Right) SETHI P-band radar image, revealing subsurface hydrological features in a very efficient way.

Acknowledgments: The author would like to thank the JAXA for providing PALSAR data in the framework of the Kyoto & Carbon Protocol project, and the ONERA for providing SETHI data in the framework of the TUNISAR project. This work was financially supported by the Centre National d'Etudes Spatiales (CNES) and by the European Space Agency (ESA).

Conflicts of Interest: The author declares no conflict of interest.

References

1. Lee, J.-S.; Pottier, E. *Polarimetric Radar Imaging: From Basics to Applications*; CRC Press: Boca Raton, FL, USA, 2009; p. 398.
2. Elachi, C.; Roth, L.E.; Schaber, G.G. Spaceborne radar subsurface imaging in hyperarid regions. *IEEE Trans. Geosci. Remote Sens.* **1984**, *GE-22*, 383–388. [[CrossRef](#)]
3. Farr, T.G.; Elachi, C.; Hartl, P.; Chowdhury, K. Microwave penetration and attenuation in desert soil: A field experiment with the Shuttle Imaging Radar. *IEEE Trans. Geosci. Remote Sens.* **1986**, *GE-24*, 590–594. [[CrossRef](#)]
4. McCauley, J.F.; Schaber, G.G.; Breed, C.S.; Grolier, M.J.; Haynes, C.V.; Issawi, B.; Elachi, C.; Blom, R. Subsurface valleys and geoarchaeology of the eastern Sahara revealed by Shuttle Radar. *Science* **1982**, *218*, 1004–1020. [[CrossRef](#)] [[PubMed](#)]
5. Paillou, P.; Grandjean, G.; Baghdadi, N.; Heggy, E.; August-Bernex, T.; Achache, J. Sub-surface imaging in central-southern Egypt using low frequency radar: Bir Safsaf revisited. *IEEE Trans. Geosci. Remote Sens.* **2003**, *41*, 1672–1684. [[CrossRef](#)]
6. Schaber, G.G.; McCauley, J.F.; Breed, C.S.; Olhoeft, G.R. Shuttle Imaging Radar: Physical controls on signal penetration and subsurface scattering in the Eastern Sahara. *IEEE Trans. Geosci. Remote Sens.* **1986**, *GE-24*, 603–623. [[CrossRef](#)]
7. Abdelsalam, M.G.; Stern, R.J. Mapping precambrian structures in the Sahara Desert with SIR-C/X-SAR radar: The neoproterozoic Keraf suture, NE Sudan. *J. Geophys. Res.* **1996**, *101*, 23063–23076. [[CrossRef](#)]
8. Farr, T.G.; Rosen, P.A.; Caro, E.; Crippen, R.; Duren, R.; Hensley, S.; Kobrick, M.; Paller, M.; Rodriguez, E.; Roth, L.; et al. The Shuttle Radar Topography Mission. *Rev. Geophys.* **2007**, *45*. [[CrossRef](#)]
9. Drake, N.A.; El-Hawat, A.S.; Turner, P.; Armitage, S.J.; Salem, M.J.; White, K.H.; McLaren, S. Palaeohydrology of the Fazzan Basin and surrounding regions: The last 7 million years. *Palaeogeogr. Palaeoclimatol. Palaeoecol.* **2008**, *263*, 131–145. [[CrossRef](#)]
10. Ghoneim, E.; El-Baz, F. The application of radar topographic data to mapping of a mega-paleodrainage in the eastern Sahara. *J. Arid Environ.* **2007**, *69*, 658–675. [[CrossRef](#)]
11. Robinson, C.A.; Werwer, A.; El-Baz, F.; El-Shazly, M.; Fritch, T.; Kusky, T. The Nubian aquifer in Southwest Egypt. *Hydrogeol. J.* **2007**, *15*, 33–45. [[CrossRef](#)]
12. Paillou, P.; Reynard, B.; Malézieux, J.-M.; Dejax, J.; Heggy, E.; Rochette, P.; Reimold, W.U.; Michel, P.; Baratoux, D.; Razin, P.; et al. An extended field of crater-shaped structures in the Gilf Kebir region—Egypt: Observations and hypotheses about their origin. *J. Afr. Earth Sci.* **2006**, *46*, 281–299. [[CrossRef](#)]
13. Rosenqvist, A.; Shimada, M.; Ito, N.; Watanabe, M. ALOS PALSAR: A pathfinder mission for global-scale monitoring of the environment. *IEEE Trans. Geosci. Remote Sens.* **2007**, *45*, 3307–3316. [[CrossRef](#)]
14. SAHARASAR. Available online: <http://saharasar.obs.u-bordeaux1.fr/> (accessed on 8 March 2017).
15. Paillou, P.; Lopez, S.; Farr, T.; Rosenqvist, A. Mapping Subsurface Geology in Sahara using L-band SAR: First Results from the ALOS/PALSAR Imaging Radar. *IEEE J. Select. Top. Earth Obs. Remote Sens.* **2010**, *3*, 632–636. [[CrossRef](#)]
16. Pachur, H.J.; Hoelzmann, P. Late Quaternary palaeoecology and palaeoclimates of the eastern Sahara. *J. Afr. Earth Sci.* **2000**, *30*, 929–939. [[CrossRef](#)]
17. Paillou, P.; Schuster, M.; Tooth, S.; Farr, T.; Rosenqvist, A.; Lopez, S.; Malézieux, J.-M. Mapping of a major paleodrainage system in Eastern Libya using orbital imaging Radar: The Kufrah River. *Earth Planet. Sci. Lett.* **2009**, *277*, 327–333. [[CrossRef](#)]
18. Paillou, P.; Tooth, S.; Lopez, S. The Kufrah Paleodrainage System in Libya: A Past Connection to the Mediterranean Sea? *C.R. Geosci.* **2012**, *344*, 406–414. [[CrossRef](#)]
19. Pachur, H.J.; Altmann, N. *Die Ostsahara im Spätquartär*; Springer: Berlin/Heidelberg, Germany; New York, NY, USA, 2006; p. 662.

20. Osborne, H.A.; Vance, D.; Rohling, E.J.; Barton, N.; Rogerson, M.; Fello, N. A humid corridor across the Sahara for the migration of early modern humans out of Africa 120,000 years ago. *Proc. Natl. Acad. Sci. USA* **2008**, *105*, 16444–16447. [[CrossRef](#)] [[PubMed](#)]
21. McGee, D.; Demenocal, P.B.; Winckler, G.; Stuut, W.; Stuur, J.B.; Bradtmiller, L.I. The magnitude, timing and abruptness of changes in North African dust deposition over the last 20,000 year. *Earth Planet. Sci. Lett.* **2013**, *371–372*, 163–176. [[CrossRef](#)]
22. Krastel, S.; Hanebuth, T.J.H.; Antobreh, A.A.; Henrich, R.; Holz, C.; Kolling, M.; Schulz, H.D.; Wien, K.; Wynn, R.B. Cap Timiris canyon: A newly discovered channel system offshore of Mauritania. *EOS Trans. Am. Geophys.* **2004**, *85*, 414–423.
23. Vörösmarty, C.J.; Fekete, B.M.; Meybeck, M.; Lammers, R.B. Global system of rivers. Its role in organizing continental land mass and defining land-to-ocean linkage. *Glob. Biogeochem. Cycles* **2000**, *14*, 599–621. [[CrossRef](#)]
24. Skonieczny, C.; Paillou, P.; Bory, A.; Bayon, G.; Biscara, L.; Crosta, X.; Eynaud, F.; Malaizé, B.; Revel, M.; Aleman, N.; et al. African Humid periods triggered the reactivation of a large river system in Western Sahara. *Nat. Commun.* **2015**, *6*. [[CrossRef](#)] [[PubMed](#)]
25. Yang, X.; Rost, K.T.; Lehmkuhl, F.; Zhenda, Z.; Dodson, J. The evolution of dry lands in northern China and in the Republic of Mongolia since the Last Glacial Maximum. *Quat. Int.* **2004**, *118*, 69–85. [[CrossRef](#)]
26. Lee, M.; Lee, K.; Lim, S.; Lee, J.; Yoon, H. Late Pleistocene–Holocene records from Lake Ulaan, southern Mongolia: Implications forecast Asian palaeomonsoonal climate changes. *J. Quat. Sci.* **2013**, *28*, 370–378. [[CrossRef](#)]
27. Komatsu, G.; Brantingham, P.; Olsen, J.; Baker, V. Paleoshoreline geomorphology of Boon Tsagaan Nuur, Tsagaan Nuur and Orog Nuur: The Valley of Lakes, Mongolia. *Geomorphology* **2011**, *39*, 83–98. [[CrossRef](#)]
28. Lehmkuhl, F.; Lang, A. Geomorphological investigations and luminescence dating in the southern part of the Khangay and the Valley of the Gobi Lakes (Central Mongolia). *J. Quat. Sci.* **2001**, *16*, 69–87. [[CrossRef](#)]
29. Sternberg, T.; Paillou, P. Mapping potential shallow groundwater in the Gobi using remote sensing: Lake Ulaan Nuur. *J. Arid Environ.* **2015**, *118*, 21–27. [[CrossRef](#)]
30. Paillou, P.; Dreuillet, P. The PYLA'01 experiment: Flying the new RAMSES P-band facility. In *AIRSAR Earth Applications Workshop*; JPL Publication: Pasadena, CA, USA, 2002.
31. Paillou, P.; Ruault du Plessis, O.; Coulombeix, C.; Dubois-Fernandez, P.; Bacha, S.; Sayah, N.; Ezzine, A. The TUNISAR experiment: Flying an airborne P-Band SAR over southern Tunisia to map subsurface geology and soil salinity. In *Proceedings of the Progress Electromagnetics Research Symposium Abstracts, Marrakesh, Morocco, 20–23 March 2011*.
32. Paillou, P.; Dubois-Fernandez, P.; Lopez, S.; Touzi, R. SAR polarimetric scattering processes over desert areas: Ksar Ghilane, Tunisia. In *Proceedings of the POLINSAR Programme, Frascati, Italy, 23–28 January 2017*.
33. Le Toan, T.; Quegan, S.; Davidson, M.; Baltzer, H.; Paillou, P.; Papathanassiou, K.; Plummer, S.; Rocca, F.; Saatchi, S.; Shugart, H.; et al. The BIOMASS mission: Mapping global forest biomass to better understand the terrestrial carbon cycle. *Remote Sens. Environ.* **2011**, *115*, 2850–2860. [[CrossRef](#)]

